PCCP

Accepted Manuscript

ROYAL SOCIETY OF CHEMISTRY

www.rsc.org/pccp

Molecular dynamics of dibenz[a,h]anthracene and its metabolite interacting with lung surfactant phospholipid bilayers

Helmut I. Padilla-Chavarría, Teobaldo R. C. Guizado, and Andre S. Pimentel*

Departamento de Química, Pontifícia Universidade Católica do Rio de Janeiro, Rua Marques de São Vicente, 225, Gávea, CP 38097, 22451-900, Rio de Janeiro, RJ, Brazil

*Corresponding author: a_pimentel@puc-rio.br

Abstract

The interaction of dibenz[a,h]anthracene and its ultimate carcinogenic 3,4-diol-1,2-epoxide with lung surfactant phospholipid bilayer was successfully performed using molecular dynamics. The DPPC/DPPG/Cholesterol bilayer (64:64:2) was used as lung surfactant phospholipid bilayer model and compared with a DPPC bilayer as reference. The dibenz[a,h]anthracene and its 3,4-diol-1,2-epoxide were inserted in the water and lipid phases in order to investigate their interactions with the lung surfactant phospholipid bilayers. The radial distribution function between two P atoms in polar heads presents that the 3,4-diol-1,2-epoxide affects the order between the P atoms in the DPPC/DPPG/Cholesterol model more than dibenz[a,h]anthracene, which is a consequence of its preference for the polar heads and dibenz[a,h]anthracene prefers to be located in the hydrocarbon chain of the phospholipid bilayer. Dibenz[a,h]anthracene and its 3,4-diol-1,2-epoxide may form aggregates in water and lipid phase, and in the water-lipid interface. The implications for the possible effect of dibenz[a,h]anthracene and its 3,4-diol-1,2-epoxide in the lung surfactant phospholipid bilayer are discussed.

Keywords: pulmonary clearance, bilayers, lung cancer, hydrocarbon polycyclic aromatic, surface tension, atmospheric pollution.

Introduction

Particulate matter air pollution plays an important role in the development of several lung diseases such as asthma, chronic obstructive pulmonary diseases, fibrosis, and lung cancer [1]. These health problems appear in environments where aerosol particles can reach high concentrations and population is exposed at long times [2]. The development of a lung disease due to aerosol inhalation is very complex [3], but the effectiveness of natural clearance processes due to overloading by deposited particles seems to play an important role in its development [4]. In such situations there are more deposited particles in the distal lung than can be removed effectively by alveolar macrophages, endocytosis and exocytosis of deposits by tissue cells, and direct hydrodynamic transport of deposits by activity of the pulmonary surfactant [5].

Particulate matter can be removed from alveoli because of the specific properties of the pulmonary surfactant. The effective particulate matter removal arises from the surface tension profile generated in the liquid lining during the breathing cycle [6,7]. Since the high activity of the surfactant is essential for this hydrodynamic transport [8-10], there must have a relationship between the quality of pulmonary surfactant and the rate of the alveolar clearance. The appropriate function of the pulmonary surfactant is also important for the clearance to stimulate activity of alveolar macrophages [11,12] and to facilitate phagocytosis due to opsonization of deposited particles [13].

The maintenance of the interfacial properties of the pulmonary surfactant is essential for normal lung function. Surfactant forms a surface-active film composed primarily of phosphatidylcholine (PC) and phosphatidylglycerol (PG) that coat the air/water hypophase covering the alveolar tissue surface. By lowering surface tension to near equilibrium during inspiration, surfactant minimizes the work of breathing. By reducing the surface tension to low values during expiration, the surfactant stabilizes the lung at low volumes and limits the tendency to develop pulmonary edema. This pulmonary surfactant system thereby allows such films to attain low surface tensions near 0 mN/m, which are required for the normal breathing process.[6,7]

Polycyclic aromatic hydrocarbons (PAHs) adsorbed on particulate matter easily penetrate into the respiratory part of human lungs. When deposited, particles interact with the hypophase covering the surface of the alveoli and bronchioli. The PAHs desorbed from particles are released into the liquid and may interact with the components of the lung surfactant. Any damage of the lung surfactant degrades the

clearance process and facilitates the penetration of particulate matter or dissolved molecules into the blood system. Thus, the PAHs may cause lung cancer,[14] but also, they are one of the reasons of cellular changes by reducing the clearance rate caused by surfactant inactivation. It was demonstrated by simultaneous experimental and simulations that benzo[a]pyrene molecules are transported into the hydrophobic part of the phospholipids bilayer. Such incorporation of the benzo[a]pyrene into the surfactant structure alters the mechanical properties and surface activity.[6,7]

An experimental study and a theoretical model [15,16] described the uptake of highly lipophilic compounds by the mucosal tissue and diffusion of them through the mucosa into the blood stream. It was showed that much longer half-times for clearance are expected for PAHs compared to less lipophilic compounds. In turn, this suggests that metabolism of these compounds will substantially contribute to clearance from the respiratory tract, yielding carcinogenic metabolites that attack DNA.[17,18] The metabolic activation of PAHs to carcinogens by cytochromes P450 has been investigated, showing that epoxide, dihydrodiol, and diol epoxide structures are carcinogenic metabolites that attack DNA.[19-22]

The pulmonary surfactant generally contains 90% of lipid, mainly phosphatidylcholine (PC) and phosphatidylglycerol (PG), and 10% of surfactant-specific proteins, known as SP-A, SP-B, SP-C, and SP-D.[23,24] The surfactant system has two different regions with respect the organization and packing of phospholipids: gel, liquid disordered and liquid-ordered phases in subphase bilayers, and liquid-expanded and liquid-condensed phases in an interfacial monolayer film. Also, it has cholesterol molecules in ordered and disordered phases in both bilayer and monolayer films. The surfactant monolayer at the air/liquid interface is the first barrier protecting the human blood system against any inhalants introduced into the lung.[23,24] PAH molecules easily diffuse throughout this lung surfactant phospholipid monolayer during the normal breathing process when it attains low surface tensions near 0 mN/m, i. e., a highly disordered and fluid phase. At this situation, PAH molecules find the surfactant phospholipid bilayers in the subphase, and subsequently, the blood, lung tissues and cells, causing cancer. Other situation is the collapse of the phospholipid monolayers into bilayers transferring the PAH molecules to the subphase.[23,24]

This investigation provides information on the molecular dynamics (MD) of dibenz[a,h]anthracene (DBahA) and its metabolites (mDBahA) into phospholipid

bilayers composed of 1,2-dipalmitoyl-sn-glycero-3-phosphocholine (DPPC), 1,2-dipalmitoyl-*sn*-3-glycero[phospho-*rac*-(1-glycerol)] (DPPG), and cholesterol. The chemical structures for these compounds are presented in Figure 1. MD is a very useful tool that has been used for studies on self-assembly of lung surfactants. The literature about applying MD to lung surfactant models is wide.[6,7,25-50] Most of the MD studies used a phospholipid monolayer as a model. Few investigations about the PAH-lung surfactant interaction indeed preferred to simulate the bilayer model.[6,7,45] Some studies are intended to investigate the formation of bilayer reservoirs from monolayer and lipid transfer between the interface and subphase.[29,30,36,38,47,50] Also, there are few investigations of the interaction of lung surfactant models with nanoparticles.[31,34,43,49] Anyway, the simulation of lung surfactant bilayer is used here because it is more reasonable for explaining the underlying fate of dibenz[a,h]anthracene and its metabolites in the lung. Once the tool is applied to the lung surfactant bilayer model, conformational and dynamic information of the system can be drawn from the analysis of the results, such as orientation, formation of aggregates, and diffusion. The aim of this paper is to understand the behavior of the dibenz[a,h]anthracene and its metabolites in the lung surfactant phospholipid bilayers models. The surfactant proteins are not included in the model in order to simplify the system.

Methodology

Parameters, structures, and models. The interaction parameters for DBahA, mDBahA, Cholesterol, and DPPG were obtained using the automated topology builder (ATP) and repository, version 1.2.[51] The DPPC force field parameters were acquired from the work by Kukol.[52] It is important to mention that the ATP program does not assign the charges correctly. Thus, the group charges for these compounds were chosen and each atom charge was adjusted to keep the total charge as zero for these charge groups. It is very well known that neutral charge groups lead to more accurate simulation results. Originally, Gromos53A6 was used to parameterize molecules and proteins, considering that this force field uses neutral groups or groups with integer charge. Thus, the charge groups obtained by ATB were reevaluated to comply with this criterion. To ensure neutral charge groups or integer charge groups, they are adjusted slightly using symmetry criteria of every charge group over its atoms. Anyway, if PME is used, the possible effects of this procedure in the simulation results are negligible.[51,53,54] All simulations were carried out using the GROMOS force field

parameter set 53A6 (Gromos53A6)[53] and the GROMACS 4.6.5 package.[54] The standard force field parameters for the single-point charge water model (SPC)[55] and for the sodium cation (Na^+)[56] were used in this work.

A reference system was obtained using a bilayer structure of 128 molecules of DPPC only, 64 by layer, from the literature.[52] The bilayer orientation in this system is standard for bilayer studies, with the polar heads oriented to the water phase, and the lipid plane parallel to the XY plane of the system. This lipid bilayer was previously equilibrated with a simulation time of 40 ns, and later inserted in the center of a box with dimensions 6.4x6.4x11.0 nm. Figure 1S in the supporting information material shows a representation of this reference system. In each side of the bilayer, 10, 20, and 40 molecules of DBahA (or mDBahA) were inserted randomly inside the box. The aqueous concentrations of solute in these systems range from 0.8 to 13×10^{-3} mol L^{-1}. Then, the box was filled with SPC water models until the density achieves 1.0 kg L^{-1}. The number of SPC water molecules was approximately 7000. This system was submitted to energy minimization and a 200 ns molecular dynamics simulation was performed in order to use the trajectories for analysis. Furthermore, the same 10, 20, and 40 molecules of DBahA (or mDBahA) were added in the lipid phase, generating higher concentrations (0.05 to 0.40 mol L^{-1}) because solute is accumulated inside the bilayer in this situation. The system was again submitted to energy minimization and a 50 ns molecular dynamics simulation was done in order to understand if these molecules would diffuse into water phase.

The bilayer structure formed by 64 DPPC, 64 DPPG, and 2 cholesterol molecules was built by using the CELLmicrocosmos 2.2.2 membrane editor package.[56] To build lipid phase with the solute molecules, the phospholipid bilayers were built using an algorithm to randomly distribute, one by one, the molecules under the *xy* plane of area 6.5 nm x 6.5 nm, sorting the exact proportion of 32 DPPC molecules, 32 DPPG molecules, 1 cholesterol molecule, and the intended number of PAH molecule by each layer. The lipid plane was put parallel to the *xy* plane of the system. The bilayer orientation was arranged in such a way to put the polar heads oriented to the water phase. This system was inserted in the center of a box with dimensions 6.5x6.5x19.0 nm. The representation of this DPPC/DPPG/Cholesterol model is shown in Figure 2. Then, 40 molecules of DBahA (or mDBahA) were randomly added in the lipid phase. The PAH concentrations for these systems are around 0.40 mol L^{-1}, accumulated inside

the bilayer. Afterwards, the box was filled with SPC water models until the density achieves 1.0 kg L^{-1}. The number of SPC water models was approximately 19000. Also, it was inserted 64 sodium cations (Na^+) to equilibrate the charges.

Molecular dynamics. For all systems, an energy minimization was performed to avoid the system collapse in the beginning of the MD. The energy minimization was done using the steepest descent algorithm until the interaction energy reaches 250 kJ mol^{-1}. The systems were put into a space-filling box, which is replicated periodically in the x, y and z directions. In the reference system starting with the DBahA (or mDBahA) in the water phase, it was done a 200 ps MD to relax the system using the leap frog algorithm.[57] The velocities were generated for all particles by using a temperature of 310 K and the Maxwell-Boltzman distribution. In the NVT ensemble, a weak thermal coupling with velocity rescaling thermostat[58] was used with 0.1 ps at 310 K. When the system was started with the DBahA (or mDBahA) inside the lipid phase, the MD was performed with 1000 ps using the NpT ensemble. The temperature coupling with velocity rescaling thermostat[58] was 0.5 ps at 310 K and the semi-isotropic pressure coupling was 2 ps at 1 bar by using the Parrinello-Rahman barostat.[59] A cut-off of 10 Å for long-distance interactions were taken into account by means of the particle mesh Ewald (PME) technique.[60] The LINCS algorithm[61] was used to reset bonds to their correct lengths after an unconstrained update.

The 200 ns MD simulations for the systems starting with DBahA (or mDBahA) in the water phase were performed to estimate the thermodynamic properties of the system using the NpT ensemble. For the same purpose, the systems with DBahA (or mDBahA) starting in the lipid phase were simulated using a 50 ns MD using the same ensemble. This last step was performed using a weak thermal coupling (τ_T = 0.1 ps) at T = 310 K and a semi-isotropic pressure coupling of τ_p = 2 ps at 1 bar by using the Parrinello-Rahman barostat.[59] The short range and long range cut-offs for non-bonded interactions were 1 nm for van der Waals interactions and 1.2 nm for Coulomb interactions. Energy dispersion corrections and neighbor list updates were taken at each 10 fs. The particle mesh Ewald (PME) technique was used with a cut-off of 10 Å for long-distance interactions.[60] The LINCS algorithm[61] was used to reset the bonds at each 2 fs. Trajectories were run up with a time step of 2 fs. All analyses were performed using the last 30 ns of the data for superficial area, thickness, diffusion, order parameter,

and radial distribution function of the film, using coordinates, velocities and energies recorded at intervals of 2 ps.

Analysis. The cluster analysis was performed with the function g_clustsize with cutoff of 0.35 nm using the last 20 ns of simulation and periodic boundary conditions. The radial distribution functions (RDFs) were calculated between different charged groups: the positively charged group is choline, essentially $N^+(CH_3)_3$, and the negatively charged one is the phosphate group, essentially PO_2O^-. The most transparent way to understand the effect of DBahA and mDBahA with the phospholipid bilayer in the ordering is to consider RDFs between nitrogen and phosphate atoms in the choline and between phosphate groups, i.e., the pair correlation behavior between these charged groups. The RDFs presented in this study are therefore for the P-P and N-P pairs. It is important to note that, as atoms itself have a volume and cannot overlap at the same position, the RDFs usually start with zero until the atom diameter is reached. Basically, the RDFs are calculated using only the *xy* plane (parallel to the membrane) due to the semi-isotropic nature of the system. The result is the RDF projection on the *xy* plane that starts with a nonzero density because there are two layers. As the atom from one layer is located at r=0, the atom from the second layer above makes a nonzero density at r=0. This RDF presents clearly the distributions independently within both the *xy* plane and the normal direction.

The MD simulations allow a thorough description of the molecular organization of the phospholipid bilayer. This is an important issue because the degree of order may be correlated with the order parameter (S_z), which is related to the average spatial orientation of molecules and may be defined as

$$S_z = \frac{1}{2}\left\langle 3\cos\theta_z - 1 \right\rangle$$

(Equation 1)

where θ_z is the angle between a reference vector in lipid molecules and the z axis and the brackets denote the average over all equivalent atoms and over time. The perpendicular direction emerges as a natural choice to compute order parameters for monolayers spreading on the *x*-*y* plane. S_z values range from -0.5 to +1.0, meaning an orientation either fully perpendicular or fully parallel to the *z* axis, respectively. A value of around 0 means an average random orientation of the vector with respect to the *z*

axis. For the aliphatic atoms, the line joining the reference atom and the next heavy atom attached to it will define the vectors.

The mean square displacement (MSD) is calculated from a set of positions. Then, the diffusion coefficient D can be obtained from the slope of the lateral mean-square displacement (MSD) versus time in the bilayer models as described below in Equation 2:

$$D = \lim_{t\to\infty} \frac{1}{2Nt} \frac{d}{dt} \left\langle \left\| r_i(t + t_0) - r_i(t_0) \right\|^2 \right\rangle_{t_0}$$

(Equation 2)

where $r_i(t)$ is the is the vector of the position for the center of mass for each molecule i and N is the dimension of the movement, i. e., N =2 for lateral diffusion and N = 1 for diffusion in the z-axis. The MSD was averaged over time and over all of the lipid molecules. The diffusion coefficient is calculated by least square fitting the MSD data from the last 30 ns. The error is estimated by the difference of the diffusion coefficients obtained from fits over two halves of the fit interval.

Results and Discussion

In this work, a mixed bilayer of DPPC, DPPG, and cholesterol is explored theoretically as lung surfactant model using MD simulations in order to understand the fate of DBahA and mDBahA interacting with this model. A well known DPPC bilayer is used as reference for comparison with the lung surfactant model above.

The temperature, pressure, and energy of all simulations were analyzed in order to verify the equilibration of the model and the reference. These verifications are shown in Figures 2S in the supporting information material. It is also important to validate the methodology by comparison with experimental results. The lateral diffusion coefficients (D) of fluorescent lipid analogs in DPPC membranes and in large DPPC vesicles are around 10^{-7} and 10^{-8} cm^2 s^{-1}, respectively.[62] Our results shows that the lateral diffusion coefficients of lipids in the pure DPPC and the DPPC/DPPG/cholesterol bilayers are $(3\pm1)\times10^{-8}$ and $(2\pm2)\times10^{-8}$ cm^2 s^{-1}, respectively. As the lateral diffusion is highly dependent of the transition phase, varying in about two orders of magnitude, we believe that our simulations are reliable because our results fall into the range cited above.

Normally, the order parameter is used to measure the level of agreement of the simulation compared with the experiment. This parameter is obtained directly from nuclear magnetic resonance measurements of selectively deuterated phospholipids. S^{CD} represents the averaged value calculated by Equation 1 using the time dependent angle θ^{CD} between the carbon-deuterium (CD) bond vector and a reference axis (normal to the plane *xy* of the bilayer). The angular brackets denote a time and ensemble average of all phospholipids during the time of analysis (last 30 ns). The value of S^{CD} is -0.5 when the hydrocarbon chain is totally ordered (solid phase). Usually, S^{CD} values of -0.2 are found for phospholipid bilayers in the fluid phase.[63] Figure 3S in the supporting information material presents the order parameter (S^{CD}) for the sn1 and sn2 hydrocarbon chains of the DPPC model with 10, 20, and 40 molecules of DBahA (or mDBahA). The results show that DBahA and mDBahA increase the order of the phospholipid chain, i. e., the phospholipid bilayer becomes less fluid as the number of DBahA (or mDBahA) molecules is raised. However, the values of $-S^{CD}$ are in agreement with those found in literature.[63] It is also observed that DBahA has larger effect than its metabolite, mDBahA, indicating that DBahA location is closer to the hydrocarbon chains and mDBahA prefers to be located in the polar head. Table 1 shows the values of $-S^{CD}$ for the sn1 and sn2 hydrocarbon chains of the DPPC/DPPG/Cholesterol model with 40

molecules of DBahA or mDBahA. The values of $-S^{CD}$ are also in agreement with those found in literature.[63] The values of $-S^{CD}$ for DPPG are slightly larger than those for DPPC in positions 2-4 in the sn1 hydrocarbon chain, and for positions 5-15, the values of $-S^{CD}$ for DPPC are slightly larger than those for DPPG interacting with molecules of DBahA (or mDBahA). In contrast, the positions 2-7 of sn2 hydrocarbon chain in the DPPG molecule have slightly larger values of $-S^{CD}$ as compared with those for DPPC interacting with molecules of DBahA (and positions 2-5 for mDBahA). The positions 8-15 of sn2 hydrocarbon chain in the DPPC molecule have a slightly larger value of $-S^{CD}$ compared with those for DPPG interacting with molecules of DBahA (and positions 6-15 for mDBahA). In general, the hydrocarbon chain of DPPG molecules is more ordered next to the polar head than that for DPPC molecules, and in the tail of the hydrocarbon chain, the DPPC molecule is more ordered than DPPG ones. The RDFs confirm the order parameter observations.

After the verifying the equilibration of reference and model, and validating the methodology by comparison with experimental results, the interactions of DBahA and mDBahA with the pure DPPC bilayer (reference) and the DPPC/DPPG/Cholesterol bilayer (model) were simulated. First, 10, 20, and 40 molecules of DBahA (or mDBahA) were placed in water phase to interact with the pure DPPC bilayer in 200 ns MD simulations. The results show that they diffuse into the lipid phase as presented in Figure 4S in the supporting information material. Thus, 10, 20, and 40 molecules of DBahA (or mDBahA) were randomly inserted in the lipid phase, and 50 ns MD simulation were performed in order to study if these molecules may be released to the water phase. As presented in Figure 5S in the supporting information material, they do not diffuse to the water phase using a 50 ns MD simulation. This observation is in agreement with the literature[7,64] that shows anthracene and benz[a]pyrene prefer the lipid phase as expected. Another study investigating PAHs in membranes with MD was carried out by Hoff et al.[65] In particular, the literature[66-68] confirms the finding of this paper that DBahA prefer being located in the lipid phase. The interactions of DBahA and mDBahA with the pure DPPC bilayer were then studied. Figure 5S and 10 S show the preferences about the location of DBahA and mDBahA molecules.

Figure 6AS in the supporting information material presents the RDF between the atoms N and P in the polar heads of the pure DPPC bilayer interacting with 10, 20, and 40 molecules of DBahA (or mDBahA). The RDF between two P atoms in the polar

heads of the DPPC bilayer in the same system is shown in the Figure 6BS in the supporting information material. The results show that DBahA and mDBahA do not affect the order between N and P atoms; however, they have more influence in the order of two P atoms. The existence of N and P atoms in the same DPPC molecule is represented by a sharper peak as compared with the RDF of two P atoms that are located in different DPPC molecules. In this latter distribution, mDBahA affects the distance of the two P atoms in greater extent compared to DBahA because the DBahA and mDBahA locations. The mDBahA molecules are located near the polar heads whereas the DBahA molecules prefer a more hydrophobic environment inside the lipid phase. Thus, the mDBahA molecules move the two P atoms away from each other. Consequently, mDBahA has more influence in the order of two P atoms than DBahA. Our previous study also shows that the drug chlorpromazine also has a major effect in the order of two P atoms.[69]

Figure 3A presents the RDF between the atoms N and P in the polar heads of the DPPC/DPPG/Cholesterol model with 40 molecules of DBahA (or mDBahA) interacting with the model. The RDF between two P atoms in the polar heads of the model with the same number of molecules is shown in the Figure 3B. The results present that DBahA and mDBahA also do not affect the order between N and P atoms although the number of N atoms in the DPPC/DPPG/Cholesterol model is half as compared with the DPPC bilayer. The peak in the DPPC/DPPG/Cholesterol bilayer (Figure 3A) is even sharper as compared with the peak in the DPPC model (Figure 6AS). The larger peak for mDBahA in the RDF between two P atoms in the polar heads of the model indicates that mDBahA also has more influence in the order of two P atoms than DBahA molecules, i. e., in the distance between the two polar heads. This is a consequence of the mDBahA preference for a position closer to the polar heads than DBahA is located in the DPPC/DPPG/Cholesterol model.

The area per phospholipid and the thickness of the DPPC bilayer are around 0.61-0.64 nm^2 and 3.87-4.38 nm, respectively, depending on the number of DBahA (or mDBahA) molecules. The thickness is calculated by using the center of mass of the phosphorus atoms from the upper and lower phospholipid layers. Table 2 summarizes the area of the system, the area per phospholipid, and the thickness of the models used in this study. It is observed that the number of DBahA (or mDBahA) molecules does not affect the area per phospholipid, but the thickness increases as the number of

DBahA (or mDBahA) molecules is raised. More specifically, the thickness is also more affected by DBahA than mDBahA ones because the first is located between the hydrocarbon chains and the other prefers to be located closer to the polar heads. The explanation for that is related to two aspects: it is easier to move away the hydrocarbon chains due to their flexibility and there is formation of aggregates inside the bilayer that modifies its thickness.

The thickness of a membrane is around 5 nm.[70] However, the DPPC bilayer has a thickness of 3.7 nm.[71] The comparison between experiment and simulation with the same force field used here for different phosphatidylcholine bilayers yields a thickness of about 3.5 nm.[72] Leekumjorn and Sum[73] found a thickness of 3.43 nm for pure DPPC using the same force field. The area per phospholipid and the thickness of the DPPC/DPPG/Cholesterol model with 40 molecules of DBahA or mDBahA inserted in the bilayer are about 0.60-0.62 nm^2 and 4.0-4.2 nm, respectively. It is noted no meaningful difference in the area per molecule and thickness between the DPPC and DPPC/DPPG/Cholesterol models. It is possible to observe that the thickness of the model with DBahA is slightly larger compared with the model with mDBahA for most of the simulation time. Our results show that the thickness calculated for the models studied here are lower than those found for membranes published in the literature,[70] but higher than those found for phosphatidylcholine bilayers.[71,72] It is important to mention that an inadequate implementation of the pressure coupling may result in lipid monolayer separation in the bilayer and an artificial translation of DBahA (or mDBahA) molecules. Therefore, it is indeed essential that the pressure does not fluctuate considerably because any artifact in this parameter may result the observation of an artificial phenomena. A way to avoid any artifact in the simulation is to choose the *z*-length of the box larger (around twice) than *x*- and *y*-lengths, and an semi-isotropic pressure coupling, i. e., the pressure coupling in the *z*-axis is independent of the pressure coupling in the xy-plane.

Figure 8S in the supporting information material presents the mean square displacement of the center of mass for DBahA and mDBahA under the *xy*-plane of the DPPC bilayer. It is observed that the lateral diffusion of DBahA is larger than for mDBahA. This is also due to the location of the molecules. Unlike mDBahA is located more closely to the polar heads, DBahA interacts more strongly with the hydrocarbon chains that has more freedom of motion than the polar heads. The same behavior for

DBahA compared to mDBahA is evidenced in the DPPC/DPPG/Cholesterol model as presented in the Figure 4A. The mean square displacement for DBahA is larger in the DPPC/DPPG/Cholesterol bilayer compared to the DPPC model. The explanation for this behavior is well established since cholesterol modifies the mechanical, thermophysical and lateral organizational properties of membranes, bringing less flexibility for bilayer but the DPPG effect on increasing flexibility of the hydrocarbon chains is more important.[69,74,75] As mDBahA is located closer to the polar head, it seems that its lateral diffusion is not affected by the presence of DPPG and cholesterol.

Figure 9S in the supporting information material presents the mean square displacement of the center of mass of DBahA and mDBahA in the z-axis of the DPPC bilayer. Figure 4B shows the mean square displacement of the center of mass of DBahA and mDBahA in the *z*-axis of the DPPC/DPPG/Cholesterol model with 40 molecules of DBahA (or mDBahA). Similarly to what occurred with the lateral diffusion, it is observed that DBahA moves quickly in the normal direction to the *xy*-plane than its metabolite, mDBahA. The explanation for this behavior is that mDBahA interacts more strongly with the polar heads than the DBahA with the hydrocarbon chains, indicating that the latter one has more freedom of motion inside the hydrocarbon chains. However, this freedom of motion does not reflect in a larger permeability, but in an easier translation between the two layers of the bilayer. It is possible to mention that the lateral movement is normally faster than diffusion in the *z*-axis. Unlike the lateral movement, it is important to note that the movement in the *z*-axis increases as the number of DBahA (or mDBahA) molecules is raised.

Figure 11S in the supporting information material presents the trajectories of 10, 20, and 40 molecules of DBahA (or mDBahA) starting in the lipid phase during 50 ns of simulation of the DPPC bilayer. It is observed that DBahA molecules prefer to be located between the hydrocarbon chains, as previously described, and some of them cross from one layer to another, but there is no transfer to the water phase. In contrast to DBahA, mDBahA molecules interact more with polar heads. The interaction is so strong that mDBahA is not transferred to the water phase and there is no crossing between layers. Figure 4 presents the trajectories of 40 molecules of DBahA (or mDBahA) during 50 ns of simulation of the DPPC/DPPG/Cholesterol model with these molecules starting in the lipid phase. The results are very similar to those found for the DPPC model and it is not interesting to repeat for sake of conciseness.

In this study, it is not observed a linear increase of the normal diffusion (between phases) with respect the initial concentration of DBahA (or mDBahA) in the water phase. Consequently, this system presents a complex behavior. The diffusion of these molecules between phases decreases as their aqueous concentrations are raised due to the formation of aggregates in the water-lipid interface. The formation of aggregates is also observed in water and lipid phases. It is important to note that the simulation time is in the order of a couple hundred nanoseconds. Nevertheless, the aggregates diffuse from water to lipid phase in longer time scales.[76] Therefore, an aggregate diffusing between phases merely moves away the phospholipid molecules found in the bilayer, creating a "hole", which is simply a region of lower density. In the lipid bilayer, the behavior is semi-isotropic and the diffusion in the *z*-axis is slower than the lateral diffusion. As there is some difficulty for the phospholipids move in the *z*-axis, its lateral diffusion is more favorable. Thus, it will be needed a larger energy than usual to occur lateral diffusion. Indeed, there is movement of aggregates, but the time of simulation is not enough to measure it and this is the explanation for the large error in the mean square displacement (MSD) presented in Figures 8S and 9S.

Figure 4S in the supporting information material shows the snap shots in 0 and 200 ns for the DPPC model with DBahA (or mDBahA) starting in the water phase. The snap shots A, B, and C are, respectively, the starting configurations (0 ns) for 10, 20, and 40 molecules of DBahA in the water phase. DBahA molecules are transferred to the lipid phase, and in 200 ns, they achieve the final snap shots D, E, and F representing the configurations for 10, 20, and 40 molecules of DBahA, respectively. The snap shot D shows that DBahA is transferred to the lipid phase without forming agglomerates. Subsequently, as the number of molecules is raised, the snap shots E and F presents an increase in the formation of aggregates, making the transfer to the lipid phase difficult. The snap shots G, H, and I are the starting configurations (0 ns) for 10, 20, and 40 molecules of mDBahA, respectively, in the water phase. The mDBahA molecules prefer to be located in the region of the polar head in 200 ns as presented in the snap shots J, K, and L. It is observed that the size of aggregates in the water-lipid interface (region of the polar head) increases as the number of mDBahA.

Figure 5 shows the snap shots in 0 and 50 ns for the DBahA and mDBahA starting in the lipid phase in the DPPC/DPPG/Cholesterol model. The snap shots 5A and 5B are the starting configurations (0 ns) for 40 molecules of DBahA and mDBahA

in the lipid phase, respectively. As previously presented for the DPPC model (Figure 11S, snap shot F), these molecules do not escape from the lipid phase as well. They achieve the final snap shots 5C and 5D representing the configurations for 40 molecules of DBahA and mDBahA, respectively. The snap shots 5C and 5D present that they form aggregates in the interior of the lipid bilayer and in the water/lipid interface, respectively. Our recent study also shows the formation of aggregates for aromatic compounds in the water-lipid interface.[77] Figure 6 shows the cluster analysis of the last 20 ns of simulation. Figure 6A shows that the number of clusters in the system is around 20. From the cluster analysis, it is possible to observe that the two or three molecules would pack around each other and clusters are representative and stable. The distribution of clusters is presented in the histogram (Figure 6B) which relates the number of molecules per cluster and the average number of clusters. The average cluster size is presented in Figure 6C. As it can be observed, the number of molecules in the cluster size seems to be practically constant and slightly higher than 2. Usually, the aggregates are formed in the interior of the membrane, but from the 200 ns MD simulation with DBahA (or mDBahA) starting in the water phase, the clusters are already formed before entering the membrane.

The formation of aggregates and its dynamics complicate the analysis comparing different concentrations of DBahA and mDBahA because the aggregates behave like a bulky compound that diffuses very slowly into the phospholipid bilayer. It is important to note that the force field used in this study does not describe π-π interactions. Thus, the formation of aggregates in this study is only lead by the interactions between DBahA (or mDBahA) molecules with itself, and with water. This latter interaction is not favorable compared the first one. In a more realistic simulation, it should be included these π-π interactions; however the force field used here can not reproduce π-π interactions for the simple reason that the force field does not describe electrons explicitly. On the other hand, it has been parameterized to reproduce average properties of small compounds and several types of different interactions can be observed.[78] In the force field used, the aromatic rings have partial charges to reproduce the delocalization of the electrons. Thus, it is not a π-π stacking interaction but an interaction between two rings that could be assimilated to a π-π interaction although it does not have explicit description of electrons or polarization. It is possible to really study those interactions in details, but it should be employed a QM/MM method in the particular system of rings,

and in this case, the more correlated wavefunction is, the better is the description. As π-π interactions are governed by electron correlation effects, there is not a potential that actually account it explicitly in the force field expression. However, a regular Lennard-Jones potential is able to capture some of the energetics of π-π interaction in the Amber force field.[79] Indeed, if the π-π interaction is included, the formation of aggregates will be enhanced in the simulation.

Implications

The dynamics of DBahA interacting with the lung surfactant phospholipid bilayers seems to be very similar to that for benzo[a]pyrene.[6,7] Therefore, it may be possible to generalize the fate of PAHs in the lung surfactant. Indeed, 4 or 5-ring PAHs should interact similarly with the lung surfactant. However, it is important to mention that some parent PAHs are weak carcinogens that require metabolism to become more potent carcinogens due to the diol epoxide metabolites produced in the metabolism, which are mutagenic and affect normal cell replication when they react with DNA to form adducts.[17,18] It is predicted that the potency of different diol epoxides is enhanced if they are in the "bay" region of the PAH molecule.[19-22] Up to date, this study seems to be the first one to predict the interaction of these metabolites inside the lung surfactant. It is also worthy to mention that their interaction may be strong enough to make them remaining for long times (>200 ns) in the polar head region of the lung surfactant phospholipid bilayers.

Due to the high hydrophobicity, DBahA and mDBahA may form aggregates in the water subphase inside the lung. However, DBahA may also form aggregates in the particulate material that is normally introduced in the respiratory system, resulting in transfer of DBahA aggregates from the particulate material to the lung surfactant. From the study performed for DPPC bilayers, whose results seem to be similar to the DPPC/DPPG/Cholesterol model, it is possible to infer that, as the number of DBahA (or mDBahA) molecules is raised, it forms more aggregates in the phospholipid bilayer, water phase, and water-lipid interface. The formation of aggregates in the water phase diminishes their transfer to the lipid phase because they are bulky to translate by the small room between two polar heads. After the aggregate is adsorbed in the water-lipid interface, several DBahA molecules from it "drip" into the lipid phase and diffuse to the interior of the phospholipid bilayer. Therefore, the diffusion is really reduced as the number of DBahA molecules is increased in the water subphase. Consequently, more

DBahA molecules in the water phase tend to form aggregates in the water-lipid phase, making easier the diffusion to the phospholipid bilayer and enhancing accumulation. As secondhand smokers inhale less DBahA molecules into the lung than active smokers, it is possible to infer that secondhand smokers are more likely to have DBahA molecules easily diffusing through the lung surfactant and accumulating inside the phospholipid bilayers in the lung subphase. The bulky aggregates may be easily eliminated by the clearance process.

Conclusion

The molecular dynamics of the interaction of DBahA and its metabolite mDBahA with lung surfactant phospholipid bilayer was successfully performed using the GROMOS force field parameter set 53A6 and the GROMACS 4.6.5 package. The lung surfactant phospholipid bilayer was modeled with a mixture of DPPC, DPPG, and cholesterol (64:64:2), and a DPPC model was used as reference. DBahA and mDBahA were inserted in the water and lipid phases in order to investigate their interactions with the lung surfactant phospholipid bilayers. The radial distribution function between N and P atoms presents that DBahA and mDBahA do not affect the order between N and P atoms in the DPPC/DPPG/Cholesterol model. However, the radial distribution function between two P atoms in the polar heads of this model indicates that mDBahA has more influence in the order of two P atoms than DBahA molecules, which is a consequence of the mDBahA preference for the polar heads. DBahA prefers to be located deeper in the hydrocarbon chain of the phospholipid bilayer. The thickness of the DPPC/DPPG/Cholesterol model is around 3.9-4.4 nm, which is within the range of experimental and theoretical thicknesses found in literature. Depending on the concentration, DBahA and mDBahA may form aggregates in water and lipid phase, and in the water-lipid interface. As the number of these molecules is raised, the formation of aggregates is enhanced. The implications for the possible effect of DBahA and mDBahA concentrations in the lung surfactant phospholipid bilayer are discussed.

Acknowledgements

The authors thank the Brazilian funding agencies CNPq (Grant No. 481481/2010-9 and 304187/2009-7), CAPES (Grant No. 02559/09-9), and FAPERJ (Grant No. E-26/101.452/2010) for financial support. T.R.C.G. also thanks CAPES for a post-doc PNPD fellowship. H. I. P. C acknowledges CNPq for a graduate fellowship.

References

1. F. H. Y. Green, V. Vallyathan, F. F. Hahn, *Toxicol. Pathol.* **2007,** 35 (1), 136-147.
2. B. Turoczi, A. Hoffer, A. Toth, N. Kovats, A. Acs, A. Ferincz, A. Kovacs, A. Gelencser, *Atmos. Chem. Phys.* **2012**, 12 (16), 7365-7370.
3. W. Stober, R. O. McClellan, *Crit. Rev. Toxicol.* **1997**, 27 (6), 539-598.
4. R. Sturm, *Comput. Biol. Med.* **2007**, 37 (5), 680-690.
5. V. I. Hof, Patrick, G. *J. Aerosol Med.*, **1994**, 7 (1), 39-47.
6. T. R. Sosnowski, M. Kolinski, L. Gradon, *Ann. Occup. Hyg.* **2011**, 55 (3), 329-338.
7. T. R. Sosnowski, M. Kolinski, L. Gradon, *J. Biomed. Nanotech.* **2012**, 8 (5), 818-825.
8. A. Podgorski, L. Gradon, *Ann. Occup. Hyg.* **1993**, 37 (4), 347-365.
9. A. Podgorski, T. R. Sosnowski, L. Gradon, *J. Aerosol Med.* **2001**, 14 (4), 455-466.
10. L. Gradon, S. E. Pratsinis, A. Podgorski, S. J. Scott, S. Panda, *J. Aerosol Sci.* **1996**, 27 (3), 487-503.
11. R. P. Baughman, D. Mangels, B. C. Corser, *Chest* **1987**, 91 (3S), S28-S28.
12. J. F. van Iwaarden, E. Claassen, S. H. M. Jeurissen, H. P. Haagsman, G. Kraal, *Am. J. Resp. Cell Mol. Biol.* **2001**, 24 (4), 452-458.
13. P. Gehr, F. H. Y. Green, M. Geiser, V. I. Hof, M. M. Lee, S. Schurch, *J. Aerosol Med.* **1996**, 9 (2), 163-181.
14. T. M. Penning, *Chem. Res. Toxicol.* **2014**, 27 (11), 1901-1917.
15. P. Gerde, P. Scholander, *Environ. Res.* **1987**, 44 (2), 321-334.
16. P. Gerde, P. Scholander, *Environ. Res.* **1989**, 48 (2), 287-295.
17. K. Donny-Clark, S. Broyde, *Nucleic Acids Res.* **2009**, 37 (21) 7095-7109.
18. Y. Cai, D. J. Patel, N. E. Geacintov, S. Broyde, *J. Mol. Biol.* **2007**, 374 (2), 292-305.

A

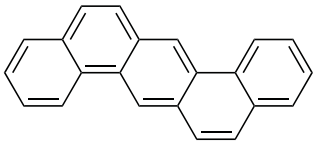

DBahA

B

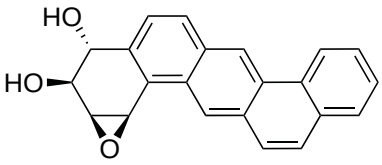

mDBahA

C

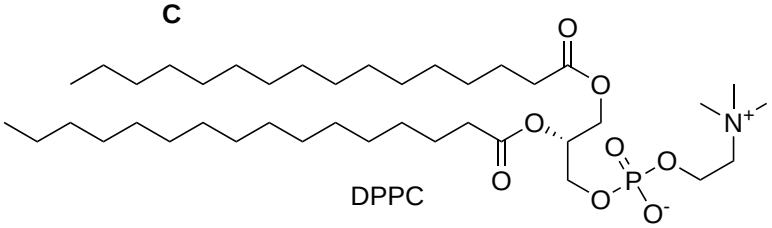

DPPC

D

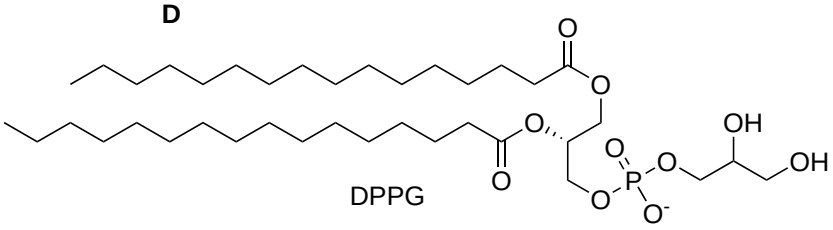

DPPG

E

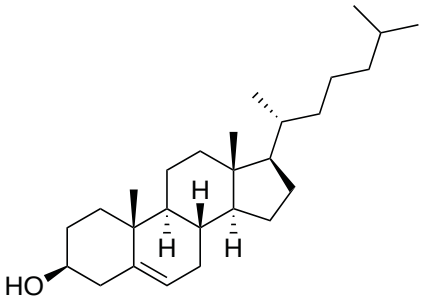

Cholesterol